



Bifunctional maleimide dyes as selective anion sensors

Zhenghuan Lin, Hung Cheng Chen, Shih-Sheng Sun*, Chao-Ping Hsu*, Tahsin J. Chow*

Institute of Chemistry, Academia Sinica, Taipei 115, Taiwan, ROC

ARTICLE INFO

Article history:

Received 6 February 2009

Received in revised form 21 April 2009

Accepted 28 April 2009

Available online 6 May 2009

Keywords:

Anion sensor

Maleimide

Fluorescence quenching

Red dye

ABSTRACT

A class of disubstituted maleimide dyes with two symmetrical NH binding sites was found to exhibit distinct color change and fluorescence quenching effect for fluoride, cyanide, and dihydrogen phosphate anions. The intense red emission displayed apparent solvatochromic shift, indicating a strong charge-transfer character. The interactions between the dyes and anions were variable depending on the amine substituents at C(3,4) of the maleimides. For the dyes with two pyrrolyl receptor sites, the NH protons were deprotonated by more basic anions such as fluoride or cyanide. For those with two indolyl receptor sites, formation of a chelate with H_2PO_4^- through hydrogen bonds played a major role.

© 2009 Elsevier Ltd. All rights reserved.

1. Introduction

Anions play crucial roles in environmental, chemical, and biological systems in forms of drugs, food additives, agricultural fertilizers, biologic metabolites, and waste liquid from chemical plants, etc.¹ Among them, cyanide, fluoride, and phosphate are of particular concerns due to their usages as raw materials in the production of nylon and resins; in the prevention of dental caries and treatment of osteoporosis; and in the signal transduction and energy storage in biological systems, respectively.² Nevertheless, these three kinds of anion have also caused huge damages on environments, such as toxic wastes, water eutrophication, and even in the production of nerve gases.³ As a consequence there is in need of sensitive and easy testing methods for detecting these anions.

Recently, fluorimetric sensors based on dipyrrolylquinoxaline (DPQ) have been reported for detecting similar anions by hydrogen bonding with pyrrole protons.⁴ However, DPQ and its simple derivatives did not exhibit satisfactory sensitivity.⁵ By integrating DPQ into a polymer backbone and coordinated with Ru(II) ion as developed by Sun et al.⁶ and Pavel et al.,⁷ the sensitivity of DPQ can be improved substantially. These efforts have mostly been focused on changing the electronic and optical properties of the quinoxaline moieties, which have led to quite complicated molecular structures.

The intense red color and high luminescent efficiency of maleimide-based fluorophores has attracted considerable attention recently.^{8,9} These series of compounds are derivatives of natural products, which can be synthesized easily in the lab. They are

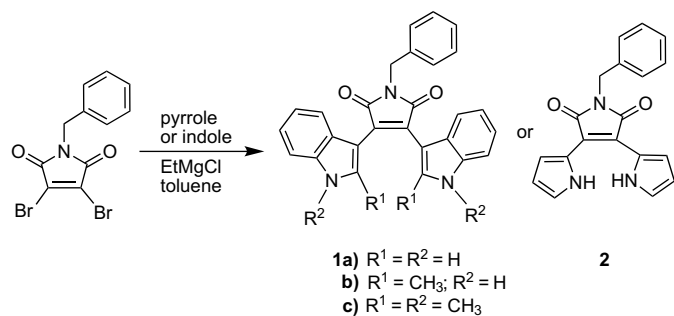
highly stable compounds, yet display remarkable long wavelength emissions both in solutions and in solid state. They have been utilized successfully on organic light-emitting diodes (OLEDs) as emitting materials⁹ and on pharmaceutical investigations as potential new drugs.¹⁰ The structure of derivatives with pyrrolyl substituents at C(3,4) positions bears a good similarity to the structural of DPQ, yet their unique red color renders them an exceptional candidate beyond DPQ.

In this paper we describe an unprecedented design of maleimide derivatives for use as effective anion sensors. The maleimide-based derivatives were chosen as the fluorophore of anion sensors for three reasons: (1) maleimide, as an electron-withdrawing group, is expected to enhance the acidity and the H-bond donor property of pyrrolyl groups. (2) The optical property of maleimide is sensitive to receptor–anion interactions, thus suitable for both colorimetric and fluorimetric detections. (3) There is an argument on the origin of fluorescence quenching of these types of sensors, i.e., either it is caused by the formation of hydrogen bonding,^{4,5,7} or simply due to the result of deprotonation.^{6,11} In this report we tried to resolve these arguments by analyzing this new type of maleimide sensors.

2. Results and discussions

Two types of maleimide derivatives were synthesized by replacing the bromide groups at C(3) and C(4) positions of *N*-benzyl-2,3-dibromomaleimide with either indoles (**1a–c**) or pyrroles (**2**) through Grignard reactions (Scheme 1). The bonding structure of pyrrolyl moieties in compounds **1a,b** is different from that in compound **2**, thus offers a chance for examining the structural effect on anion sensing properties. Compound **1c** does not have any free –NH

* Corresponding authors. Tel.: +886 2 27898552; fax: +886 2 27884179.
E-mail address: tjchow@chem.sinica.edu.tw (T.J. Chow).



Scheme 1. Synthesis of compounds **1a–c** and **2**.

moiety, therefore is not suitable for using as sensors. Nevertheless its relatively lower pH dependency in the absorption and higher quantum efficiency in the emission rendered it a more appropriate model for the analysis of solvatochromic effect.

Compounds **1a–c** and **2** exhibit three major absorption bands in the range of 250–550 nm region (Fig. 1 and Fig. S1). They are known to derive from π – π^* transitions, where the lower energy ones at λ_{\max} 455–520 nm exhibit a significant charge-transfer character.^{8,12} Each molecule contains a pair of cross-intercepted dipoles, which consist of an electron donor (pyrrole) and an electron acceptor (maleimide carbonyl). Electron transition from HOMO to LUMO thus generated a charge-separated state. An apparent solvent effect can be seen in both the absorption and emission spectra of **1c** (S1). In its absorption spectrum, the lowest energy band is red-shifted from 460 nm in cyclohexane to 480 nm in acetonitrile. The high energy band at 283 nm, however, is not influenced by the solvents. Upon photo-excitation, a broad featureless band appeared at λ_{\max} 575–610 nm, which changes both its intensity and wavelength in different solvents. A substantial red shift and reduction of intensity appeared along with the increase of solvent polarity. Similar spectral patterns were also found in compounds **1a**, **1b**, and **2** (Fig. 1 and Figs. S2 and S3). The charge-transfer band in **2** is red-shifted to a greater extent comparing to those of **1a–c**. A list of their spectroscopic parameters is given in Table 1.

The qualitative evaluation of the anion sensing capability of **1a**, **1b**, and **2** was performed in dichloromethane solutions containing a series of anions, namely, F[−], Cl[−], Br[−], I[−], H₂PO₄[−], HSO₄[−], NO₃[−], OAc[−], and CN[−]. Among them highly selective sensory properties were found for F[−], CN[−], and H₂PO₄[−] anions. In the presence of fluoride ion, the color of solutions **1a**, **1b**, and **2** changed along with significant fluorescence quenching. The cyanide ion can be detected in

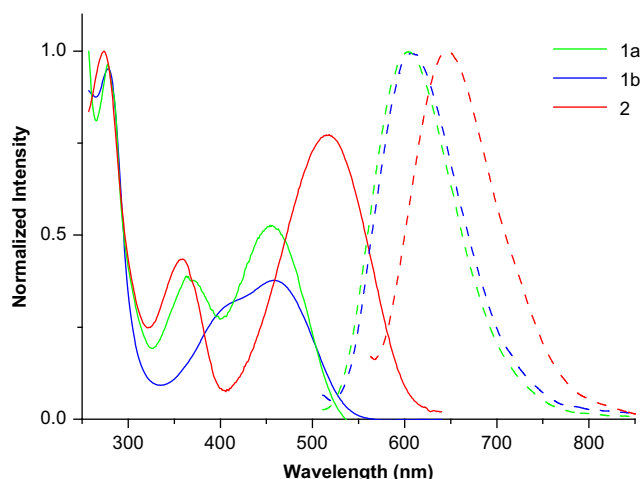


Figure 1. Optical absorption (solid lines) and luminescence (dashed lines) spectra of **1a**, **1b**, and **2**.

Table 1
Spectroscopic parameters of compounds **1a**, **1b**, and **2** in CH₂Cl₂ and their binding constants toward anions K (M^{−1})

	1a	1b	2	DPQ ^a
λ_{abs}^b (nm)	456 (560)	459 (595)	517 (584)	—
λ_{em}^b (nm)	610	616 (650)	653 (715)	—
Φ_{em} (%)	35	2	7	—
K (F [−])	3.91×10^3	6.19×10^2	1.85×10^4	1.82×10^4
K (H ₂ PO ₄ [−])	3.99×10^3	1.53×10^3	<100	60
K (CN [−])	<50	<50	3.63×10^4	220
K (other anions)	<50	<50	<50	—

Data in parentheses correspond to the anions.

^a Data obtained from Ref. 7.

^b The lowest energy band.

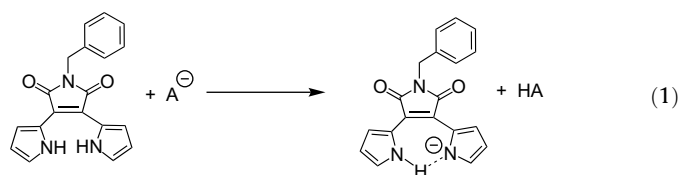
the same way by using **2**; and dihydrogen phosphate ion by using **1a** and **1b**.

The visual colors of compounds **1a** and **2** in the presence of different anions exhibit clear distinctions (S4, S5). The yellow emission of dilute solutions (50 μ M) of **1a** in dichloromethane was quenched by the addition of F[−] and H₂PO₄[−] ions, yet persisted upon the addition of other anions. The red emission of compound **2** exhibited similar quenching effect for F[−] and CN[−], but unaffected by H₂PO₄[−] ion. The relative intensities of fluorescence are shown as bar charts in Figure 2 for a better comparison.

A typical titration curve of fluoride by **2** is shown in Figure 3. The long wavelength absorption at λ_{\max} 516 nm decreased in the presence of fluoride along with the increasing of 580 nm band. A distinct isosbestic point can be detected at 542 nm, indicating the formation of a stable new species. Another isosbestic point at 414 nm was observed simultaneously as a result of increasing the 362 nm band. In the emission spectrum of **2**, the intensity of 646 nm band decreased gradually along with the increased concentration of fluoride ion. For instance, in the presence of 25 molar equivalence of fluoride ion, the emission intensity of **2** reduced to <10% of the original level. Compounds **1a** and **1b** behave similarly toward fluoride ion, i.e., a red-shift in the absorption spectra and a quenching of fluorescence (S6, S9).

The sensory properties of **1a** and **2** were selective between cyanide and dihydrogen phosphate ions. In the presence of cyanide ion, compound **2** showed a color change from red to blue, quite similar to what observed for fluoride ion. The absorption band at λ_{\max} 580 nm increased along with a decrease of the 516 nm band (S11). The red fluorescence at 646 nm was effectively quenched by cyanide ion. Compounds **1a,b** did not exhibit any interaction with cyanide ion, but showed significant fluorescence quenching with dihydrogen phosphate (Fig. 4 and Fig. S7). It is clear that the anion sensing interactions of compounds **1a,b** are not quite the same as that of **2**. Both the distance and relative orientation between the two NH groups must have played an important role.¹³

In the presence of fluoride ion the emission of **2** was quenched (Fig. 3), yet along with an apparent red shift of the spectrum. A weak new band centered at ca. 705 nm cannot be ignored, and is likely to have derived from the emission of the anion of **2**. The relatively stronger basicity of fluoride and cyanide anions can abstract a proton from the pyrrole of **2** to yield a mono-anion with stable cyclic structure (Eq. 1). The emissive property of this anion is further examined by DFT analysis.



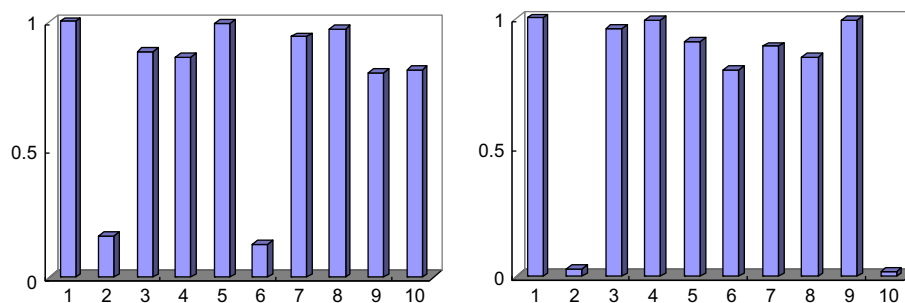


Figure 2. (Left) Bar chart indicating the relative intensity of fluorescence of **1a** (10 μM) at 604 nm in the presence of different anions (2 mM). (Right) Relative fluorescence intensity of **2** (10 μM) at 646 nm in the presence of different anions (2 mM). Anions arranged from left to right: 1-none, 2-F⁻, 3-Cl⁻, 4-Br⁻, 5-I⁻, 6-H₂PO₄⁻, 7-HSO₄⁻, 8-NO₃⁻, 9-OAc⁻, and 10-CN⁻.

In order to confirm the spectral nature of the anion, compound **2** was treated with a strong base N(Et)₄OH in dichloromethane, and its absorption and emission spectra were recorded (S12). In the presence of excess amount of base, indeed a new absorption band appeared at 584 nm and a new emission band at 715 nm. The wavelength of these transitions complies well with the new bands observed while treated with fluoride and cyanide ions (Fig. 3 and Fig. S11). It is therefore concluded that the reaction between **2** and anions was mainly acid–base in nature, and not necessarily involved a direct association of the two.¹⁴

The bonding nature of **1a,b** with anions was different from that of **2**. Their active response to H₂PO₄⁻, but not to CN⁻ as a stronger base, cannot be ascribed solely to acidity. The spectra of anionic form of **1a,b** can be obtained by the addition of N(Et)₄OH to their solutions. In the presence of excess base, the absorption spectra of **1a** and **1b** display distinctive low energy bands at 560 and 595 nm (Fig. 4 inset, S8 and S10), respectively. These spectral features were totally different from those obtained when **1a,b** were treated with either F⁻ or H₂PO₄⁻. Even for the same dye, the spectral responses to F⁻ and H₂PO₄⁻ were also different. For example, when **1a** was treated with H₂PO₄⁻, the long wavelength absorption at 455 nm diminished along with the increase of peak at 474 nm (S7). Yet when it was treated with F⁻, the new peak appeared at 504 nm (S6). Moreover, the anion of **1b** exhibited a weak emission centered at 650 nm (inset in Fig. 4), which did not appear upon reacting with either F⁻ or H₂PO₄⁻. All these information revealed that the interactions of **1a,b** with the anions must involve a direct association with each other.

The selectivity of anion recognition in the presence of other anions was also examined by a series of competitive tests. The results indicated that the sensing effect of either F⁻ or H₂PO₄⁻ by **1a** was not influenced by the presence of other anions (S13). The anion

recognition of **2**, however, was disturbed by the presence of certain anions, e.g., HSO₄⁻ or OAc⁻ (S14, S15), yet not by others all. The disturbance may be caused by a competition for proton among all the anions.

The binding stoichiometry of **1a,b** with both F⁻ and H₂PO₄⁻ was determined by Job plots and was found to be 1:1. However, their binding geometries cannot be resolved unambiguously, as indicated by the fuzzy isosbestic points in their titration spectra (Fig. 4 inset, S6, S7, and S9). Earlier reports on diindolylquinoxaline (DIQ) have shown that extended polymeric structures may exist in the association reaction with dihydrogen phosphate.¹³ A more flexible bonding conformation of these complexes rendered them difficult for crystallization.

The association constants were estimated by using the emission quenching data and the results are given in Table 1. The binding strength of **1a,b** with F⁻ ($K=0.6\text{--}3.9\times 10^3$) is slightly lower than that with H₂PO₄⁻ ($K=1.5\text{--}4.0\times 10^3$). The slightly lower affinity of H₂PO₄⁻ with **1b** than that with **1a** may be ascribed to a steric hindrance imposed by the methyl substituents of indoles. The K values of **1a,b** with H₂PO₄⁻ are about two orders of magnitude than that with DPQ (1.8×10^4).

The physical nature of molecule **2** was further confirmed by computational models based on the density functional theory (DFT) with the three-parameter Becke-style hybrid functional (B3LYP) and the 6-31G(d) basis set for geometry optimizations. In the neutral form of **2** at ground state, the two pyrrolyl rings are twisted from each other forming a significant dihedral angle of 42°. When deprotonated it formed a mono-anion, with the two pyrrolyl rings coplanar with the central ring of maleimide (Fig. 5). Such a planar conformation is favored by the formation of a cyclic 7-member ring through H-bonding as depicted in Eq. 1. The high stability of the ring structure rendered **2** more acidic than both **1a** and **1b**.

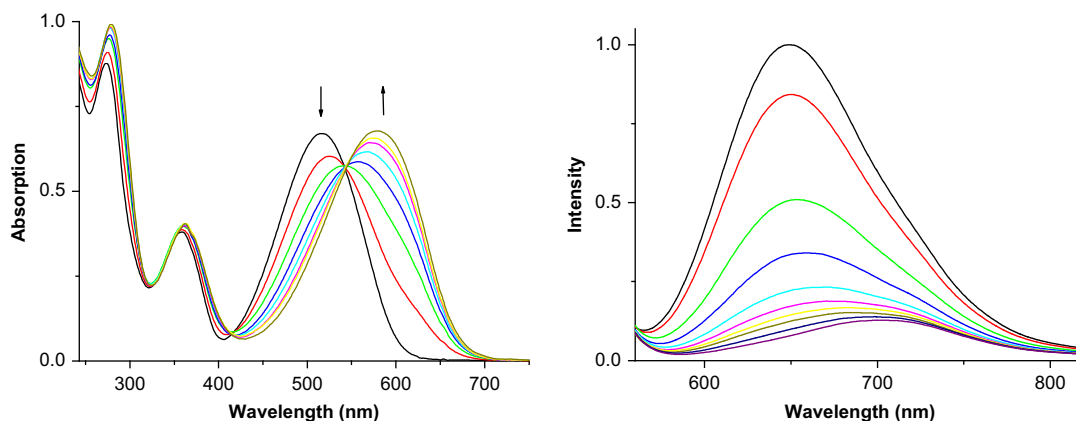


Figure 3. Absorption (left) and fluorescence (right) spectra of **2** (10 μM) upon the addition of F⁻ (0–0.25 mM in CH₂Cl₂). In the absorption spectra isosbestic points were observed at 542 and 414 nm. Fluorescence spectra were taken by irradiating at 542 nm.

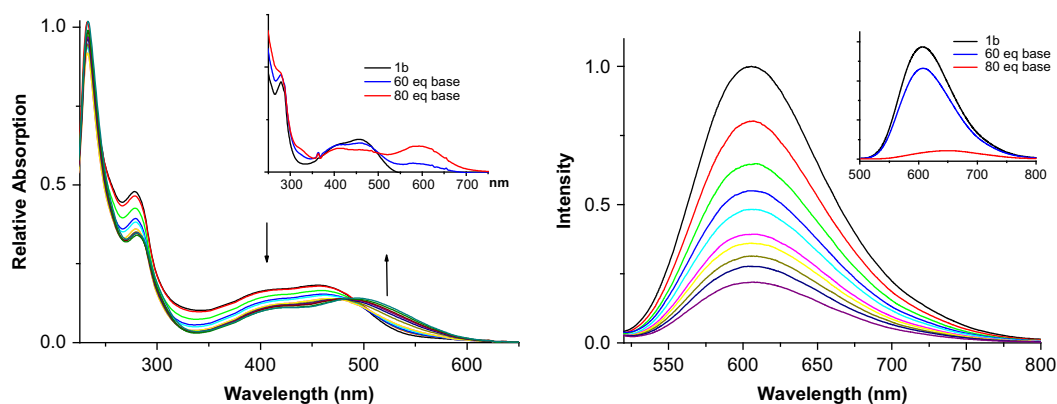


Figure 4. Absorption (left) and fluorescence (right) spectra of **1b** (10 μ M) upon the addition of H_2PO_4^- (0–2.5 mM in CH_2Cl_2). Fluorescence spectra were taken by irradiating at 486 nm. Inset in the absorption spectrum indicates the changes upon the addition of $\text{N}(\text{Et})_3\text{OH}$.

The spectra of **2** and its mono-anion were simulated by TDDFT in both the gas phase and under an external electric field to mimic the polarity of solvent. The wavelengths, worked out by an image charge approximation (ICA), correlated remarkably well with the experimental data (Table 2 and Tables T1–T4). For example, a simulated wavelength for the absorption of **2** at 496 nm fits well to the experimental value of 517 nm, and that of **2**[−] at 592 nm fits to the experimental value of 584 nm. For the emission spectra, the calculated value of wavelength for **2**[−] at 718 nm not only matches nicely with the fluorescence observed at 715 nm (Fig. 3), but also explains its weak intensity by a small value of oscillator strength (0.0187). Thus the computational results provided a strong support for an acid–base type interaction of **2** with both F^- and CN^- .

The charge-transfer nature of the electronic transitions of **2** and its mono-anion are better illustrated by the drawings of molecular orbitals. The electron density distributions of HOMO and LUMO can be depicted in Figure 6. As expected the electron density in the HOMO of **2** is mainly populated on the two symmetrically equivalent pyrrolyl moieties, while the LUMO is localized on the central maleimide moiety. Such an electronic configuration does not change much for the anion **2**[−] when **2** is deprotonated. The planar conformation of the anion should have an effect of enhancing charge delocalization across the separated rings in the ground state as well as in the excited state. As a result a narrower band gap is predicted, that is indeed verified by the longer wavelengths in both the absorption and emission spectra of the anion.

A final check on the feasibility of forming a 1:1 complex between **1a** and H_2PO_4^- was explored by B3LYP with 6–31G basis set. From the optimized structure in Figure 7, that a 1:1 association of the two is plausible in dilute solutions. The two indolyl N–H groups chelate the phosphate forming a comfortable geometry at a potential minimum. It certainly does not rule out the possibility of forming other

types of binding geometries, such as the extended structures in DIQ in more concentrated solutions or condensed phases.

In summary, bifunctional maleimide derivatives with indolyl groups (**1a** and **1b**) and pyrrolyl groups (**2**) were found colorimetric sensitive to certain anions. However, the color changing mechanisms of **1a,b** and **2** are not the same. The sensing property of **2** was based on an acid–base reaction, while a stable mono-anion of **2** formed in the presence of a stronger base. However, the spectroscopic characteristics of **1a,b** did not comply with the formation of anions while reacting with either F^- or H_2PO_4^- . Theoretical estimation by B3LYP/6–31G supported the association of 1:1 complexes in dilute solutions. The association constants of **1a,b** with dihydrogen phosphate are measured in the proximity of $\sim 10^3$, which is better than literature reported values of DPQ and DIQ.

3. Experimental

3.1. General

^1H and ^{13}C NMR spectra were recorded using Bruker AVA300 spectrometer. The chemical shifts (δ , ppm) are referenced to tetramethylsilane (TMS) as an internal standard. Mass spectra were taken on a Joel JMS 700 double-focusing spectrometer, facilitated with fast atom bombardment (FAB) for sample ionization. Microanalyses were completed on a Perkin–Elmer 2400 elemental analyzer. UV–vis absorbance spectra were recorded using a Hewlett–Packard 8453 spectrophotometer. Fluorescence spectra were recorded using a Hitachi F-4500 fluorescence spectrometer. All starting materials and solvents were obtained from commercial suppliers, e.g., *N*-benzyl-2,3-dibromomaleimide was obtained from Aldrich Chemicals. Dilute solutions used for all photophysical experiments were prepared in spectroscopic grade solvents. Thin layer chromatography

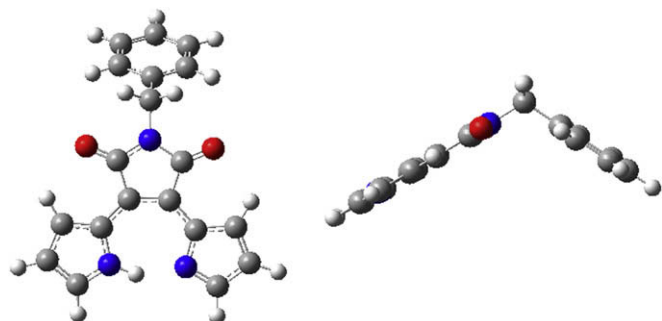


Figure 5. Optimized geometry of the mono-anion of **2**. Side view shows the coplanar conformation of the two pyrrole rings and the maleimide ring.

Table 2

Calculated parameters for the lowest transitions of compound **2** and its anion, using TDDFT/B3LYP with 6–31G(d) basis set. Simulations are performed in the gas phase and under an external electric field

TDDFT		Compound 2		Mono-anion of 2	
		Absorption	Emission	Absorption	Emission
Gas phase	eV (nm) ^a	2.54 (488)	2.25 (551)	2.11 (587)	1.95 (637)
	f_1^b	0.1922	0.1837	0.173	0.1638
ICA ^c	eV (nm) ^a	2.50 (496)	2.28 (543)	2.09 (592) ^d	1.73 (718)
	f_1^b	0.1617	0.1223	0.1444	0.0187

All other transitions are between S_0 and S_1 .

^a Transition energy.

^b Oscillator strength.

^c Image charge approximation (ICA) as an external electric reaction field.

^d $S_0 \rightarrow S_3$ as the most probable transition.

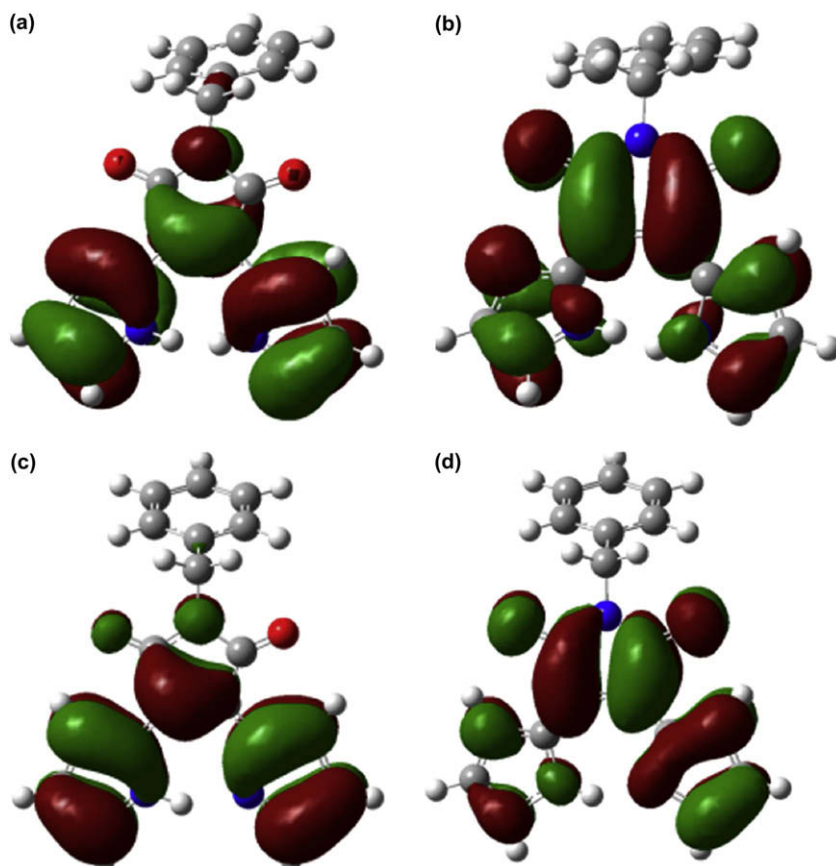


Figure 6. Frontier MOs of **2** and its anion. (a) HOMO and (b) LUMO of **2**; (c) HOMO and (d) LUMO of 2^- .

was performed on MERCK Silica Gel 60 thick layer plates. Column chromatography was performed on Sorbent Technologies brand silica gel (40–63 μm , Standard grade). The association constants, K , were determined by using the software SPECFIT 3.0 from Spectrum Software Associates, which employs a global system with expanded factor analysis and Marquardt least-squares minimization to obtain globally optimized parameters.

Geometry optimizations were completed according to the density functional theory (DFT) using B3LYP/6-31G(d) settings. For approximated structures of vibrationally relaxed LE state (emission state), they were optimized on their S1 surface at the CIS/6-31G(d) level. For the excited state parameters, time-dependent density functional theory (TDDFT) with the B3LYP/6-31G(d) settings was employed. The image charge approximation (ICA), which was used

to simulate an external electric reaction field, was performed according to our previous published procedure.¹⁵ All analyses were performed by using the Q-Chem 3.0 package.

3.2. 2,3-Bis(3-indolyl)-*N*-benzylmaleimide (**1a**)

A similar procedure to the preparation of **1b** was employed from indole and *N*-benzyl-2,3-dibromomaleimide. Compound **1a** was obtained as orange powders in 70% yield. Anal. Calcd for $\text{C}_{27}\text{H}_{19}\text{N}_3\text{O}_2$: C, 77.68; H, 4.59; N, 10.07. Found: C, 77.70; H, 4.92; N, 9.75. ^1H NMR (CD_3COCD_3 , 300 MHz): δ 4.85 (s, 2H), 6.62 (t, $J=7.6$ Hz, 2H), 6.93 (d, $J=8.1$ Hz, 2H), 7.02 (t, $J=7.6$ Hz, 2H), 7.28–7.47 (m, 7H), 7.90 (s, 2H), 10.87 (s, 2H). ^{13}C NMR (CD_3COCD_3 , 75 MHz): δ 41.27, 106.62, 111.52, 119.55, 121.46, 121.89, 125.91, 127.33, 127.41, 127.89, 128.50, 129.16, 136.38, 137.78, 171.65. HRMS (FAB) m/z $[\text{M}]^+$ calcd 417.1477, found 417.1478.

3.3. 2,3-Bis(2'-methyl-3-indolyl)-*N*-benzylmaleimide (**1b**)

To a toluene (10 mL) solution of 2-methylindole (0.85 g, 6.5 mmol) was added EtMgCl (3 M in THF, 2.16 mL) at room temperature under a nitrogen atmosphere, and the solution was heated to 45 °C for 45 min. A solution of *N*-benzyl-2,3-dibromomaleimide (0.50 g, 1.45 mmol) in toluene (10 mL) was then added to the above solution, which was heated to reflux for 12 h. The solution was cooled to room temperature and diluted with ethyl acetate (20 mL). The solution was successively washed with 1 N aqueous HCl (30 mL), water (30 mL), and brine (30 mL). It was then dehydrated over anhydrous MgSO_4 and dried in vacuo, forming a dark red residue. The crude product was purified by column chromatography with EA/hexane (1:3) as the eluant, affording compound **1b** in 75% yield (0.48 g). Anal. Calcd for $\text{C}_{29}\text{H}_{23}\text{N}_3\text{O}_2$: C, 78.18; H, 5.20; N, 9.43.

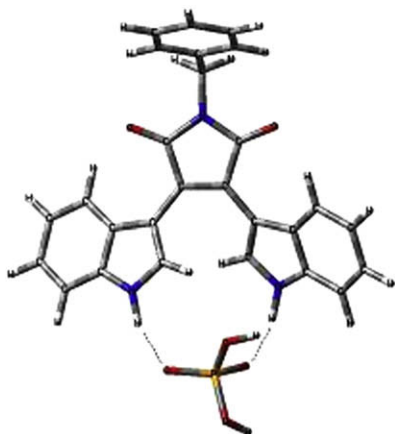


Figure 7. Optimized structure (B3LYP/6-31G) of **1a**... H_2PO_4^- complex.

Found: C, 78.17; H, 5.09; N, 9.43. ^1H NMR (CD_3COCD_3 , 300 MHz): δ 2.10 (s, 6H), 4.86 (s, 2H), 6.77 (t, $J=7.3$ Hz, 2H), 6.96 (t, $J=7.3$ Hz, 2H), 7.14 (d, $J=7.9$ Hz, 2H), 7.26 (d, $J=7.9$ Hz, 2H), 7.35 (m, 1H), 7.40 (t, $J=7.3$ Hz, 2H), 7.49 (d, $J=7.3$ Hz, 2H), 10.59 (s, 2H). ^{13}C NMR (CD_3COCD_3 , 75 MHz): δ 13.52, 42.15, 105.02, 111.33, 120.28, 120.70, 121.97, 128.01, 128.15, 128.70, 129.38, 132.59, 136.84, 138.26, 138.70, 171.88. HRMS (FAB) m/z [M] $^+$ calcd 445.1790, found 445.1782.

3.4. 2,3-Bis(2-pyrrolyl)-N-benzylmaleimide (2)

A similar procedure to the preparation of **1b** was employed from pyrrole and *N*-benzyl-2,3-dibromomaleimide. Compound **3** was obtained as dark purple solids in 10% yield. Anal. Calcd for $\text{C}_{19}\text{H}_{15}\text{N}_3\text{O}_2$: C, 71.91; H, 4.76; N, 13.24. Found: C, 72.31; H, 4.92; N, 12.76. ^1H NMR (CD_3COCD_3 , 300 MHz): δ 4.75 (s, 2H), 6.35 (dt, $J=2.6$, 4.1 Hz, 2H), 7.01 (td, $J=2.6$, 1.2 Hz, 2H), 7.29–7.40 (m, 7H), 10.40 (s, 2H). ^{13}C NMR (CD_3COCD_3 , 75 MHz): δ 41.06, 109.85, 113.57, 118.86, 122.31, 122.92, 127.42, 127.72, 128.51, 137.19, 171.85. HRMS (FAB) m/z [M] $^+$ calcd 317.1164, found 317.1158.

Acknowledgements

This work was supported by both the National Science Council and Academia Sinica of The Republic of China.

Supplementary data

Spectra of solvent shifts of **1a**, **1c**, and **2** (S1–S3). Absorption and fluorescence spectra of **1a** with F^- , H_2PO_4^- , and OH^- (S6–S8), **1b** with F^- and OH^- (S9, S10), **2** with CN^- and OH^- (S11, S12). Photographs of solutions of **1a** and **2** with a series of anions (S4, S5). Competitive tests of **1a** with F^- in the presence of other anions (S13), and those of **2** with F^- and CN^- in the presence of other anions (S14, S15). Computational results of photophysics of dye **2** using TDDFT B3LYP/6-31G(d) basis set with image charge approximation (ICA) as external electric reaction field (Tables T1–T4). Supplementary data associated with this article can be found in the online version, at doi:10.1016/j.tet.2009.04.090.

References and notes

- (a) *Riegel's Handbook of Industrial Chemistry*, 9th ed.; Kent, J. A., Ed.; Van Nostrand Reinhold-International Thomson: New York, NY, 1992; (b) *Supramolecular Chemistry of Anions*: Bianchi, A., Bowman-James, K., Garcia-España, E., Eds.; Wiley-VCH: New York, NY, 1997; pp 147–215; (c) *Ullmann's Encyclopedia of Industrial Chemistry*, 6th ed.; Bailey, J. E., Bohner, M., Brinker, C. J., Cornils, B., Evans, T., Greim, H., Hegedus, L. L., Heitbaum, J., Keim, W., Kleemann, A., Kreysa, G., Lolliger, J., McGuire, J. L., Mitsutani, A., Plass, L., Stephanopoulos, G., Werner, D., Woditsch, P., Yoda, N., Eds.; Wiley VCH: New York, NY, 1999; 1999 Electronic Release; (d) Beer, P. D.; Gale, P. A. *Angew. Chem., Int. Ed.* **2001**, *40*, 486–516; (e) Amendola, V.; Esteban-Gomez, D.; Fabbri, L.; Licchelli, M. *Acc. Chem. Res.* **2006**, *39*, 343–353.
- (a) Miller, G.C.; Pritsos, C.A. Unresolved Problems with the Use of Cyanide in Open Pit Precious Metal Mining. In *Proceedings of Cyanide: Social, Industrial and Economic Aspects*, The Minerals, Metals & Materials Society Annual Meeting, New Orleans, Louisiana, February 12–15, 2001; (b) Wiseman, A. *Handbook of Experimental Pharmacology XX/2, Part 2*; Springer: Berlin, 1970; (c) Kirk, K. L. *Biochemistry of the Halogens and Inorganic Halides*; Plenum: New York, NY, 1991; (d) Stryer, L. *Biochemistry*, 4th ed.; W.H. Freeman: New York, NY, 1995.
- (a) Dreisbuch, R. H. *Handbook of Poisoning*; Lange Medical: Los Altos, CA, 1980; (b) Kulig, K. W. *Cyanide Toxicity*; U.S. Department of Health and Human Services: Atlanta, GA, 1991; (c) Baird, C.; Cann, M. *Environmental Chemistry*; Freeman: New York, NY, 2005.
- (a) Black, C. B.; Andrioletti, B.; Try, A. C.; Ruiperez, C.; Sessler, J. L. *J. Am. Chem. Soc.* **1999**, *121*, 10438–10439; (b) Anzenbacher, P., Jr.; Try, A. C.; Miyajii, H.; Jursikova, K.; Lynch, V. M.; Marquez, M.; Sessler, J. L. *J. Am. Chem. Soc.* **2000**, *122*, 10268–10272; (c) Mizuno, T.; Wei, W. H.; Eller, L. R.; Sessler, J. L. *J. Am. Chem. Soc.* **2002**, *124*, 1134–1135; (d) Sessler, J. L.; Maeda, H.; Mizuno, T.; Lynch, V. M.; Furuta, H. *J. Am. Chem. Soc.* **2002**, *124*, 13474–13479; (e) Sessler, J. L.; Maeda, H.; Mizuno, T.; Lynch, V. M.; Furuta, H. *Chem. Commun.* **2002**, 862–863; (f) Pohl, R.; Aldakov, D.; Kubst, P.; JursTkovS, K.; Marquez, M.; Anzenbacher, P., Jr. *Chem. Commun.* **2004**, 1282–1283; (g) Anzenbacher, P., Jr.; Jursikova, K.; Aldakov, D. M.; Pohl, R. *Tetrahedron* **2004**, *60*, 11163–11168; (h) Ghosh, T.; Maiya, B. G.; Wong, M. W. *J. Phys. Chem. A* **2004**, *108*, 11249–11259.
- (a) Dmitry, A.; Pavel, A., Jr. *Chem. Commun.* **2003**, 1394–1395; (b) Dmitry, A.; Pavel, A., Jr. *J. Am. Chem. Soc.* **2004**, *126*, 4752–4753.
- Wu, C. Y.; Chen, M. S.; Lin, C. A.; Lin, S. C.; Sun, S. S. *Chem.—Eur. J.* **2006**, *12*, 2263–2269.
- Pavel, A., Jr.; Daniel, S. T.; Karolina, J.; Felix, N. C. *J. Am. Chem. Soc.* **2002**, *124*, 6232–6233.
- (a) Kaletas, B. K.; Mandl, C.; Zwan, G.; Fanti, M.; Zerbetto, F.; De Cola, L. D.; Konig, B.; Williams, R. M. *J. Phys. Chem. A* **2005**, *109*, 6440–6449; (b) Kaletas, B. K.; Joshi, H. C.; van der Zwan, G.; Fanti, M.; Zerbetto, F.; Goubitz, K.; De Cola, L.; Konig, B.; Williams, R. M. *J. Phys. Chem. A* **2005**, *109*, 9443–9445.
- (a) Yeh, T. S.; Chow, T. J.; Tsai, S. H.; Chiu, C. W.; Zhao, C. X. *Chem. Mater.* **2006**, *18*, 832–839; (b) Chiu, C. W.; Chow, T. J.; Chuen, C. H.; Lin, H. M.; Tao, Y. T. *Chem. Mater.* **2003**, *15*, 4527–4532; (c) Chan, L. H.; Lee, Y. D.; Chen, C. T. *Macromolecules* **2006**, *39*, 3262–3269; (d) Wu, W. C.; Yeh, H. C.; Chan, L. H.; Chen, C. T. *Adv. Mater.* **2002**, *14*, 1072–1075; (e) Chow, T. J.; Tsai, S. H.; Chiu, C. W.; Yeh, T. S. *Synth. Met.* **2005**, *149*, 59–62.
- (a) Nishizuka, Y. *Nature* **1984**, *308*, 693–698; (b) Mahboobi, S.; Eibler, E.; Koller, M.; Kumar, K. S.; Schollmeyer, A. P. *J. Org. Chem.* **1999**, *64*, 4697–4704; (c) Mahboobi, S.; Dechant, I.; Reindl, H.; Pongratz, H.; Popp, A.; Schollmeyer, D. *J. Heterocycl. Chem.* **2000**, *37*, 307–329.
- (a) Lin, T.-P.; Chen, C.-Y.; Wen, Y.-S.; Sun, S.-S. *Inorg. Chem.* **2007**, *46*, 9201–9212; (b) Chen, C.-Y.; Lin, T.-P.; Chen, C.-K.; Lin, S.-C.; Tseng, M.-C.; Wen, Y.-S.; Sun, S.-S. *J. Org. Chem.* **2008**, *73*, 900–911; (c) Boiocchi, M.; Boca, L. D.; Gmez, D. E.; Fabbri, L.; Licchelli, M.; Monzani, E. *J. Am. Chem. Soc.* **2004**, *126*, 16507–16514; (d) Gunnlaugsson, T.; Kruger, P. E.; Jensen, P.; Pfeffer, F. M.; Hussey, G. M. *Tetrahedron Lett.* **2003**, *44*, 8909–8913; (e) Costero, A. M.; Bañuls, M. J.; Aurell, M. J.; Ward, M. D.; Argent, S. *Tetrahedron* **2004**, *60*, 9471–9478; (f) Liu, B.; Tian, H. *J. Mater. Chem.* **2005**, *15*, 2681–2686; (g) Wu, J. S.; Zhou, J. H.; Wang, P. F.; Zhang, X. H.; Wu, S. K. *Org. Lett.* **2005**, *7*, 2133–2136; (h) Costero, A. M.; Sanchis, J.; Gil, S.; Sanz, V.; Williams, J. A. G. *J. Mater. Chem.* **2005**, *15*, 2848–2853; (i) Cho, E. J.; Moon, J. W.; Ko, S. W.; Lee, J. Y.; Kim, S. K.; Yoon, J.; Nam, K. C. *J. Am. Chem. Soc.* **2003**, *125*, 12376–12377; (j) Esteban-Gómez, D.; Fabbri, L.; Licchelli, M. *J. Org. Chem.* **2005**, *70*, 5717–5720; (k) Lee, J. Y.; Cho, E. J.; Mukamel, S.; Nam, K. C. *J. Org. Chem.* **2004**, *69*, 943–950.
- (a) Kosower, E. M.; de Souza, J. R. *Chem. Phys.* **2006**, *324*, 3–7; (b) ter Steege, D. H. A.; Burma, W. J. *J. Chem. Phys.* **2003**, *118*, 10944–10955; (c) Climent, T.; González-Luque, R.; Merchán, M. *J. Phys. Chem. A* **2003**, *107*, 6995–7003; (d) Peng, Q.; Lu, Z.; Huang, Y.; Xie, M.; Xiao, D.; Zou, D. *J. Mater. Chem.* **2003**, *13*, 1570–1574.
- (a) Sessler, J. L.; Cho, D.-G.; Lynch, V. J. *J. Am. Chem. Soc.* **2006**, *128*, 16518–16519; (b) Chen, C.-L.; Chen, Y.-S.; Chen, C.-Y.; Sun, S.-S. *Org. Lett.* **2006**, *8*, 5053–5056; (c) Chen, C.-L.; Lin, T.-P.; Chen, Y.-S.; Sun, S.-S. *Eur. J. Org. Chem.* **2007**, 3999–4010.
- Steiner, T. *Angew. Chem., Int. Ed.* **2002**, *41*, 48–76.
- Chen, H.-C.; Hsu, C.-P. *J. Phys. Chem. A* **2005**, *109*, 11989–11995.